Molecular interactions and metal binding in the theophylline-binding core of an RNA aptamer

GRANT R. ZIMMERMANN,[1,3] **CATHERINE L. WICK,**[1] **THOMAS P. SHIELDS,**[1,4]
ROBERT D. JENISON,[2,5] **and ARTHUR PARDI**[1]

[1]Department of Chemistry and Biochemistry, University of Colorado at Boulder, Boulder, Colorado 80309-0215, USA
[2]NeXstar Pharmaceuticals Inc., Boulder, Colorado 80301, USA

ABSTRACT

An RNA aptamer containing a 15-nt binding site shows high affinity and specificity for the bronchodilator theophylline. A variety of base modifications or 2′ deoxyribose substitutions in binding-site residues were tested for theophylline-binding affinity and the results were compared with the previously determined three-dimensional structure of the RNA–theophylline complex. The RNA–theophylline complex contains a U6-A28-U23 base triple, and disruption of this A28-U23 Hoogsteen-pair by a 7-deaza, 2′-deoxy A28 mutant reduces theophylline binding >45-fold at 25 °C. U24 is part of a U-turn in the core of the RNA, and disruption of this U-turn motif by a 2′-deoxy substitution of U24 also reduces theophylline binding by >90-fold. Several mutations outside the "conserved core" of the RNA aptamer showed reduced binding affinity, and these effects could be rationalized by comparison with the three-dimensional structure of the complex. Divalent ions are absolutely required for high-affinity theophylline binding. High-affinity binding was observed with 5 mM Mg^{2+}, Mn^{2+}, or Co^{2+} ions, whereas little or no significant binding was observed for other divalent or lanthanide ions. A metal-binding site in the core of the complex was revealed by paramagnetic Mn^{2+}-induced broadening of specific RNA resonances in the NMR spectra. When caffeine is added to the aptamer in tenfold excess, the NMR spectra show no evidence for binding in the conserved core and instead the drug stacks on the terminal helix. The lack of interaction between caffeine and the theophylline-binding site emphasizes the extreme molecular discrimination of this RNA aptamer.

Keywords: aptamer; H-bonds; metal binding; NMR; RNA; theophylline; U-turn

INTRODUCTION

In vitro selection (SELEX) has been used to identify RNA aptamers that bind a variety of small molecules with high affinity and specificity (Ellington & Szostak, 1990; Tuerk & Gold, 1990; Gold et al., 1995; Osborne & Ellington, 1997; Wilson & Szostak, 1999). Numerous three-dimensional structures of such RNA–ligand complexes have been reported in recent years (Dieckmann et al., 1996; Fan et al., 1996; Jiang et al., 1996; Yang et al., 1996; Zimmermann et al., 1997; Jiang & Patel, 1998). In these intricately folded structures, the nucleotides required for ligand binding are highly ordered and are often engaged in noncanonical base pairs and unusual structural motifs (Feigon et al., 1996; Heus, 1997; Patel, 1997). The specific conformations of these motifs form the basis of the ligand binding and recognition in these RNA aptamers.

In vitro selection from a random sequence library was previously used to identify RNA aptamers that tightly bind the small bronchodilator theophylline (Fig. 1A), while simultaneously discriminating against the highly similar molecule caffeine (Jenison et al., 1994). Sequence analysis of these RNA aptamers revealed a 15-nt core motif that is required for theophylline binding. This motif is represented by the box in Figure 1B,C, that also show the sequences of the RNA constructs used in this study. We previously determined the three-

A

Theophylline   Caffeine

B

Δ-33 RNA   ΔTCT-4 RNA   Δ-40 RNA   Δ-31 RNA

$K_d \cong 0.32 \ \mu M$ $K_d \cong 0.29 \ \mu M$ $K_d \cong 2.5 \ \mu M$ $K_d \cong 5.0 \ \mu M$
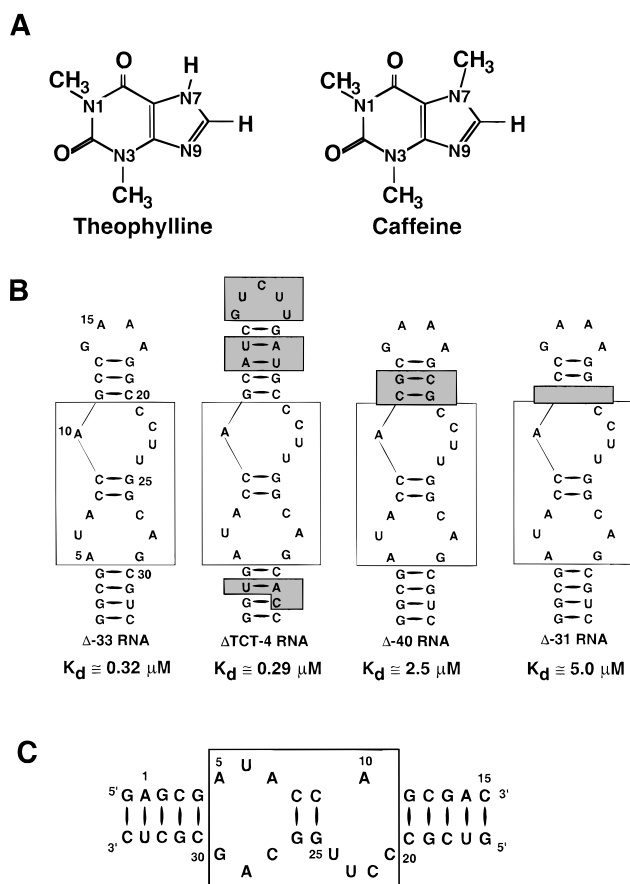
C

FIGURE 1. **A**: Covalent structures of the xanthine derivatives theophylline and caffeine. The only difference between these ligands is the methyl group at the N7 position of caffeine. **B**: Secondary structures and theophylline-binding constants (25 °C) for various constructs of the theophylline-binding RNA. Residues conserved for ligand binding are enclosed by the box; as previously discussed, residue 27 is semiconserved and can be a C or an A (Jenison et al., 1994; Zimmermann et al., 1998). The shaded regions indicate the differences between each sequence and the Δ-33 RNA construct used in the NMR studies. The numbering system used throughout the manuscript refers to the Δ-33 construct. **C**: The two-stranded construct employed in the theophylline binding measurements of the various base or sugar modifications. The numbering corresponds to that for the Δ-33 construct.

dimensional structure of the RNA–theophylline complex by solution NMR techniques and showed that the conserved residues in the core fold into a highly ordered structure integrating the theophylline ligand (Zimmermann et al., 1997). The complex contained a variety of structural motifs where many nucleotides in the binding site were involved in multiple interactions that helps explain the high level of conserved nucleotides observed in the original in vitro selection experiments. To better understand the molecular basis of the high affinity and specificity of this RNA for theophylline, various base or 2′ deoxyribose sugar modifications in the binding site of RNA–theophylline were synthesized here and tested for binding affinity. In addition, several base mutations outside the conserved core were shown to

reduce theophylline binding. The effects of these base or sugar modifications on theophylline binding are compared with the three-dimensional structure of the complex, to help understand the molecular basis of the affinity and specificity of this RNA for theophylline.

This RNA aptamer requires divalent metal ions for high-affinity theophylline binding (Jenison et al., 1994). Theophylline binding to the RNA aptamer was measured with various divalent or lanthanide ions, and high-affinity theophylline binding was only observed for the divalent ions Mg^{2+}, Mn^{2+}, and Co^{2+}. A metal-binding site was located in the ligand-binding core of the RNA (folded in the presence of 2 mM Mg^{2+}) by titrating a sample of the complex with substoichiometric amounts of paramagnetic Mn^{2+}. Finally, the hallmark of this RNA aptamer is its ability to distinguish theophylline from the highly similar molecule caffeine (Fig. 1A). No significant interactions between caffeine and the conserved nucleotides of the theophylline-binding RNA were detected by ^{1}H-NMR spectroscopy.

RESULTS

Theophylline-binding affinities for RNA variants

Theophylline-binding affinities were measured by the equilibrium-filtration procedure (Jenison et al., 1994) for a variety of RNAs containing sequence variations, or base or sugar modifications. The equilibrium-binding constants at 25 °C of four different RNA constructs are shown in Figure 1B. The ΔTCT-4 RNA has essentially the same sequence and binding affinity as the RNA used in the previous ligand-binding studies (Jenison et al., 1994), but the hairpin loop in this RNA was found to be susceptible to metal-catalyzed cleavage in the Mg^{2+}-containing buffer (not shown). Thus other RNA constructs were designed that contained stable GAAA hairpin loops (Heus & Pardi, 1991; Jucker et al., 1996) and tested for theophylline binding. Surprisingly, the Δ-31 and Δ-40 RNA constructs exhibited significantly reduced theophylline-binding affinity (Fig. 1B). The Δ-33 construct exhibited full theophylline-binding affinity, relative to the original ΔTCT-4 RNA (Fig. 1B), and was used in the previous structure determination (Zimmermann et al., 1997) and the NMR studies here.

A 2′-deoxy walk for nucleotides in the core of the theophylline-binding RNA was conducted to identify 2′ hydroxyls that are required for high-affinity ligand binding, using the two-stranded construct shown in Figure 1C. Only the 2′-hydroxyl of U24 was found to have a significant effect (Table 1) on theophylline binding. Two 7-deaza, 2′-deoxy base modifications at positions G26 or A28 were synthesized, and the theophylline-binding affinities of these modifications decreased by factors of 2 and >35, respectively (relative to binding of the 2′-deoxy modification at this position; see Table 1).

TABLE 1. Equilibrium constants for theophylline binding to various modified RNA aptamers.

Residue	Mutation	K_d (μM)
Wild-type (Δ-33 RNA)	—	0.21
A5	2'-deoxy	0.44
U6	2'-deoxy	0.50
A7	2'-deoxy	0.40
C8	2'-deoxy	0.38
C9	2'-deoxy	0.37
A10	2'-deoxy	0.33
C21	2'-deoxy	0.51
C22	2'-deoxy	0.35
U23	2'-deoxy	0.43
U24	2'-deoxy	>20
G25	2'-deoxy	0.34
G26	2'-deoxy	0.97
G26	7-deaza, 2'-deoxy	2.0
C27	2'-deoxy	0.21
A28	2'-deoxy	0.43
A28	7-deaza, 2'-deoxy	>20
G29	2'-deoxy	0.42

The binding constants were measured on wild-type and modified two-stranded RNA constructs (Fig. 1C) in 100 mM HEPES (pH 7.3), 50 mM NaCl, and 5.0 mM MgCl$_2$ at 25 °C using the equilibrium-filtration method as described in Materials and methods.

FIGURE 2. Binding curves for the RNA–theophylline complex in the presence of different divalent metals at pH 6.8, 25 °C (see text). Binding data for the Δ-33 RNA (Fig. 1B) in 5 mM Mg^{2+}, Mn^{2+}, or Co^{2+} are shown as the open triangles, open circles, and filled squares, respectively. The solid lines represent the best fit to a 1:1 complex, and the calculated K_ds for theophylline binding in the presence of the different metal ions are given. Note that theophylline binding for this RNA is pH dependent with weaker binding at pH < 7 (Zimmermann et al., 1998); thus the K_d values in this figure differ slightly from those in Table 1 because of the differences in pH.

A metal-binding site in the RNA–theophylline complex

The in vitro selection for the theophylline-binding RNA was performed in 5 mM Mg^{2+}, and this RNA motif has an absolute requirement for divalent ions to achieve high-affinity binding (Jenison et al., 1994). The theophylline-binding affinity is reduced by ~10^4 ($K_d \sim$ 4.0 mM) in the absence of divalent ions (G.R.Z. & A.P., unpubl.). To investigate the metal-ion specificity of the Δ-33 RNA (Fig. 1B), the K_ds for theophylline binding were measured (at 25 °C) for various metal ions. The results demonstrate high-affinity theophylline binding in the presence of either 5 mM Mn^{2+}, Co^{2+}, or Mg^{2+} with an order of affinity of Mn^{2+} > Co^{2+} > Mg^{2+} (see Fig. 2). Note that the binding affinity for theophylline is slightly reduced in the presence of Mg^{2+} under these conditions (pH = 6.3) because, as previously discussed (Zimmermann et al., 1998), there is a significant pH dependence for theophylline binding of this RNA construct because of the formation of a A27H$^+$-C7 base pair. More basic conditions could not be used for these studies with different metals because of the low solubility of some divalents and lanthanides at basic pH. No significant binding (K_d > 50 μM) was observed at pH = 6.3 in the presence of 5 mM Ba^{2+}, Ca^{2+}, Co(NH$_3$)$_6^{3+}$, La^{3+}, Ce^{3+}, or Gd^{3+}. Binding studies were also performed in the presence of a variety of other lanthanides, and no measurable binding of theophylline was observed. However, the low solubility of these metal ions near neutral pH likely helped contr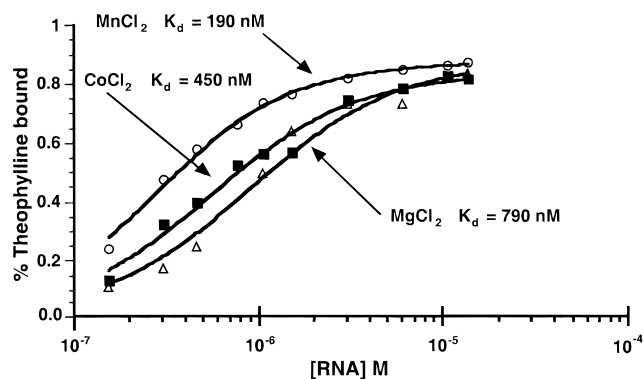ibute to the low theophylline-binding affinity under our conditions. The requirement for particular metal ions suggests that there is a specific metal-binding site in the core of this RNA aptamer.

Because Mn^{2+} satisfies the divalent metal-ion requirement of this aptamer, paramagnetic Mn^{2+}-induced relaxation of specific NMR resonances was used to identify metal-binding site(s) in the RNA–theophylline complex. After folding the complex in 2 mM free Mg^{2+}, potential metal-binding sites were identified by observing broadening of individual cross peaks in two-dimensional (^{13}C, ^{1}H) HSQC NMR spectra upon titration of the complex with substoichiometric amounts of paramagnetic Mn^{2+}. Figure 3 shows the C1'-H1'/C5-H5 region of HSQC spectra of the RNA–theophylline complex in the absence or presence of 40 μM added Mn^{2+}. The strong magnetic moment of the unpaired electron of the Mn^{2+} leads to rapid dipolar relaxation of nuclear spins in the vicinity of the metal ion (Bertini & Luchinat, 1986). Figure 3 shows that the C1'-H1' cross peaks of residues C22 and U23 are differentially broadened by Mn^{2+}. The C4'-H4' cross peaks of residues C22, U23, and U24 are broadened as a result of their proximity to a metal-binding site. The C5-H5 cross peaks of residues C3, C30, and C33 are also broadened by the Mn^{2+}, and these residues are close to the G2·U32 pair (Fig. 1B). G·U wobble pairs have been previously identified as metal-binding sites in the acceptor stem of tRNA (Ott et al., 1993) and in the cleavage-site helix of the group-I ribozyme (Allain & Varani, 1995). Mn^{2+}-induced broadening was also observed for resonances in the GAAA tetraloop of this RNA–theophylline complex, indicating a metal-binding site in this tetraloop (not shown).
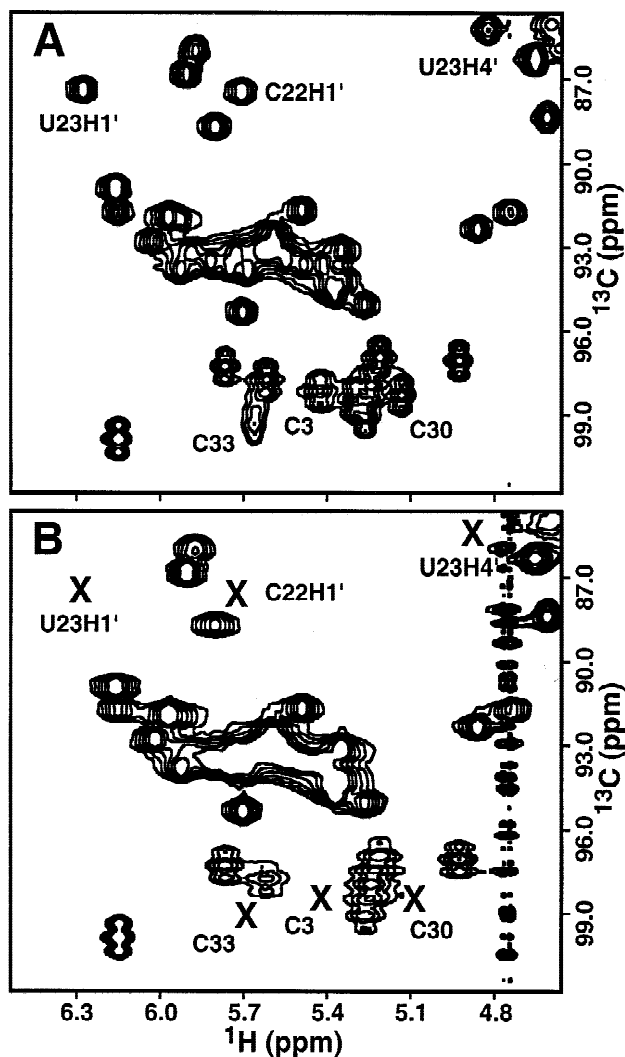
FIGURE 3. **A**: The H1′-C1′ and H5-C5 region of a two-dimensional (^{13}C,^{1}H) HSQC spectrum of the RNA–theophylline complex at 25 °C in buffer containing 2 mM MgCl$_2$. **B**: The same region after the addition of 40 μM MnCl$_2$. The crosses denote peaks that appear in **A** and are specifically broadened in the presence of paramagnetic Mn^{2+}, demonstrating these resonances are close to a Mn^{2+}-binding site.
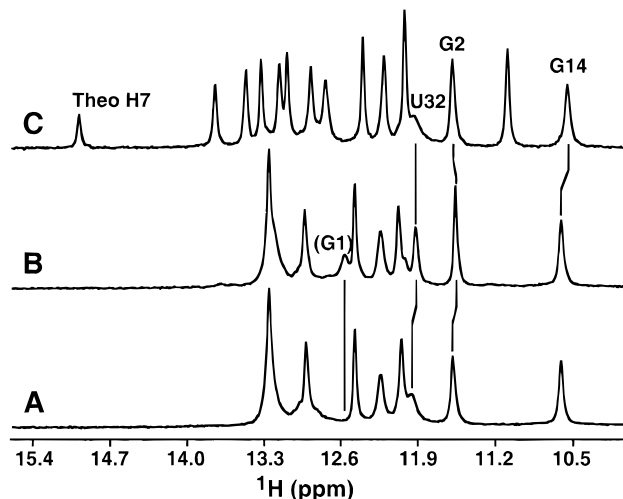

FIGURE 4. One-dimensional ^{1}H-NMR spectra of the theophylline-binding RNA (Δ-33) at 25 °C showing the effect of various ligands on the imino proton region of the spectra: **A**: no ligand; **B**: 10 equivalents of caffeine; **C**: one equivalent of theophylline.

Caffeine binding to the theophylline-binding RNA

To observe how caffeine interacts with the theophylline-binding RNA, a one-dimensional ^{1}H NMR spectrum of the RNA was collected in the presence of a tenfold molar excess of caffeine. Figure 4A,B,C shows ^{1}H NMR spectra of the RNA alone, RNA with tenfold excess caffeine, and 1:1 RNA–theophylline complex, respectively. There is relatively little change in the imino proton spectrum upon addition of caffeine, especially in comparison with the spectrum of the RNA–theophylline complex. Because the theophylline-binding RNA has a K_d of ~4 mM for caffeine (Jenison et al., 1994), it was expected that ~70% of the RNA would be bound under these conditions. However, none of the exchangeable

imino proton resonances of the theophylline-binding core nucleotides are observed in the RNA–caffeine sample. The only spectral changes in the presence of excess caffeine are a small upfield shift of the G2 imino proton, a sharpening of the U32 imino proton resonance, and a new resonance at 12.6 ppm (Fig. 4). The chemical shift of the new resonance is consistent with a guanine imino proton, and is likely the imino proton of G1. These results suggest that caffeine is stacking with the terminal helix of the RNA and is not interacting stably with the theophylline-binding core of the aptamer.

DISCUSSION

Nucleotides flanking the core can affect theophylline binding

Various aptamers were constructed containing the theophylline-binding core motif to determine which systems were suitable for NMR studies, and their ligand-binding affinities were measured at 25 °C. The hairpin-loop region of the original ΔTCT-4 theophylline-binding RNA (Jenison et al., 1994) was observed to cleave over time in Mg^{2+}-containing buffer (not shown); therefore other constructs (Fig. 1B) containing the conserved core nucleotides and a stable GAAA-tetraloop motif were synthesized. The sequence of the terminal stem was also changed in these constructs relative to the wild-type ΔTCT-4 sequence to improve transcription and for compatibility with the sequence requirements for hammerhead ribozyme cleavage that was used to post-transcriptionally process the theophylline-binding RNAs to give a homogeneous 3′ end (see Materials and methods).

The Δ-33 RNA contains a GAAA tetraloop with a flanking 3-bp stem connected to the conserved core, and this RNA has the same binding affinity for theophylline as the original wild-type ΔTCT-4 sequence. The Δ-31 construct (Fig. 1B) eliminates a single G·C pair adjacent to the theophylline-binding core, thus reducing the size of the RNA. Comparative sequence analysis of the original in vitro selection experiment indicated that only 2 bp were required to close the upper stem (Jenison et al., 1994). However, the Δ-31 construct binds theophylline with a factor of ~15 lower affinity than the wild-type ΔTCT-4 RNA (Fig. 1B). This suggests that the GAAA tetraloop and the theophylline-binding core may need to be separated by a minimum number of helical residues so that the tetraloop does not affect the structure and/or dynamics of the core. The Δ-40 construct binds theophylline with approximately eight times lower affinity than the original ΔTCT-4 aptamer or the Δ-33 construct (Fig. 1B). This result was very surprising because this RNA has the same sequence as Δ-33, except for a flip of 2 bp in the hairpin stem flanking the conserved core region. In the structure of the Δ-33 RNA–theophylline complex, the G11 stacks on top of A10 within the core region of the complex (Zimmermann et al., 1997). Thus flipping the G11-C20 pair replaces a stable purine–purine stack with a less stable pyrimidine–purine stack and may be the reason for the lower binding affinity for the Δ-40 construct. All possible base pair sequences were observed at this position in the original selection experiment (Jenison et al., 1994), indicating that the isolates from in vitro selections contain a range of binding activities, and quantitative experiments are required to define more precisely the functionally important positions.

Functional group interference mapping is consistent with a U-turn

U-turns are a common structural motif in RNA and are stabilized by intraturn base-backbone H-bonding interactions (Quigley & Rich, 1976; Jucker & Pardi, 1995). U24 is part of a U-turn in the core of this RNA aptamer (Zimmermann et al., 1997) where the U24 2′-hydroxyl is hydrogen bonded to the N7 of G26 (Fig. 5A). As seen in Table 1, replacement of the U24 2′-hydroxyl with 2′-deoxy strongly inhibits the ability of the RNA to bind theophylline (>90-fold lower affinity), presumably by disrupting this U24 2′OH-to-G26 N7 H-bond. However, disruption of this H-bond by the 7-deaza, 2′-deoxy G26 base modification has a much smaller effect on theophylline binding. The effect of the 7-deaza substitution is most appropriately addressed by comparing relative binding affinities of 7-deaza, 2′-deoxy G26 to 2′-deoxy G26 (Table 1), where the 7-deaza then results in only a twofold lower binding affinity. This might seem inconsistent with the proposed U24 2′-OH-to-G26 N7 H-bond; however, it more likely reflects the heterogeneity of

hydrogen-bonding interactions that are possible in RNAs (Jucker et al., 1996). Because the 2′ OH group represents both a H-bond donor and acceptor, upon modification of the N7 position, the U24 2′ OH can still form a H-bond with the amino group of G26. The 2′OH therefore switches from a hydrogen-bond donor to a H-bond acceptor. This type of heterogeneity of H-bonding interactions in the U-turn motif has been previously characterized in GNRA tetraloops (Jucker et al., 1996), and the data here reemphasize the heterogeneity of interactions that can be used to stabilize RNA structure. Thus the modification-interference data are consistent with formation of the U-turn in the theophylline-binding core of the RNA aptamer.

A greater than 45-fold decrease in theophylline-binding affinity was also observed for the 7-deaza, 2′-deoxy A28 mutation (relative to the 2′-deoxy modification). This 7-deaza modification disrupts the unusual U6-A28-U23 base triple (Fig. 5B) that forms the floor of the theophylline-binding site (Zimmermann et al., 1997). By disrupting the hydrogen bond with the imino proton of U23, the 7-deaza, 2′-deoxy A28 mutation destabilizes the interaction between the upper and lower loops of the RNA (Fig. 1B) and severely inhibits theophylline binding.

Table 1 also shows the effect of a set of single 2′-deoxy mutations on theophylline binding. In the solution structure of the RNA–theophylline complex, many of the 2′-hydroxyls in the core are not involved in any intramolecular interactions (Zimmermann et al., 1997), and thus would not be expected to be critical for high-affinity binding. Some other 2′-hydroxyls in the core are poised to make intramolecular H-bonds; for example, the 2′-hydroxyls of A7, C21, C22, U24, and G26 all have reasonable distances for intramolecular H-bonds in the structure of the RNA–theophylline complex (Zimmermann et al., 1997). However, only the U24 2′-deoxy substitution has a >2.5-fold effect on theophylline binding. The other 2′-hydroxyls either form similar H-bonds in the theophylline-free and theophylline-bound RNAs, form weak "context dependent" H-bonds as proposed in GNRA tetraloops by Turner and coworkers (Santa Lucia et al., 1992), or form alternate H-bonding interactions when a specific H-bond donor or acceptor is eliminated, as proposed here for the 7-deaza, 2′-deoxy G28 variant, and as previously observed in the GNRA tetraloops (Jucker et al., 1996). These data indicate that even in this highly conserved theophylline-binding core, there still exists a fair degree of flexibility for intramolecular interactions at the 2′-hydroxyl positions of the RNA.

A metal-binding site in the core of the complex

The RNA–theophylline complex requires >1 mM of certain divalent ions (Mg^{2+}, Mn^{2+}, or Co^{2+}) for high-affinity binding (Jenison et al., 1994; Fig. 2), suggesting that
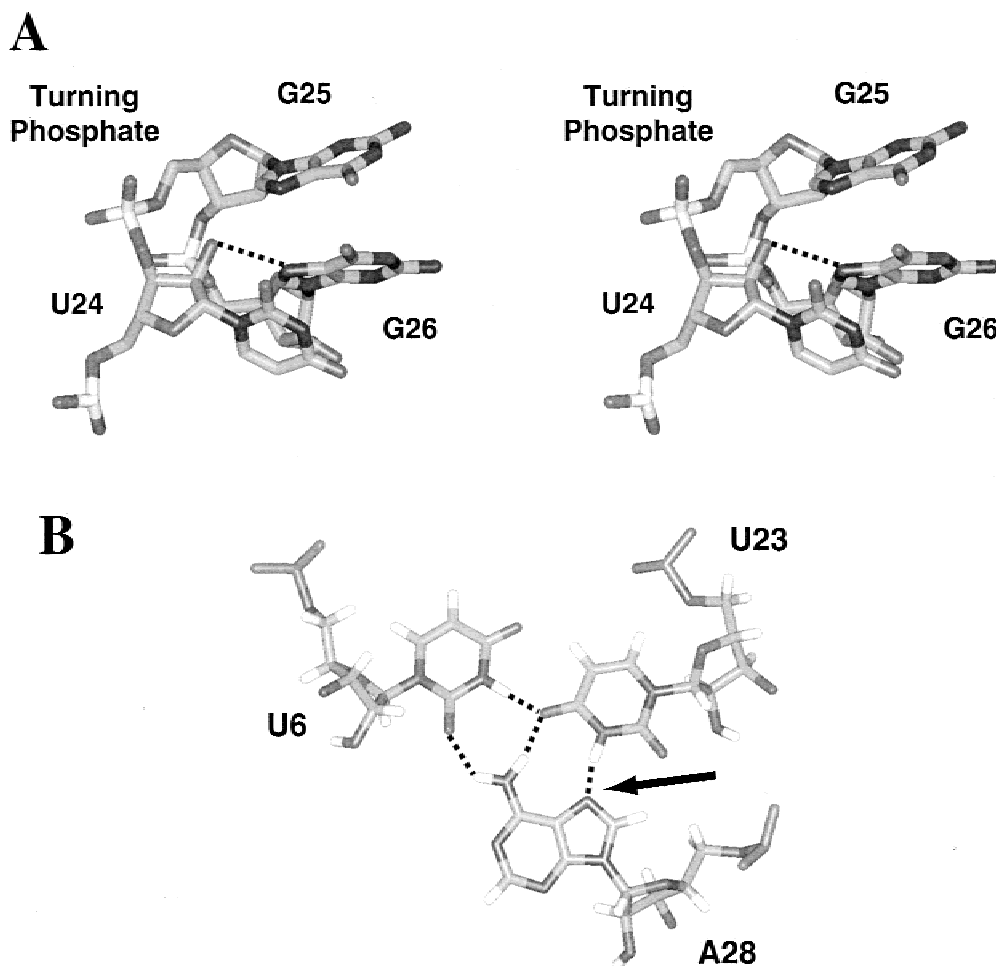
FIGURE 5. A: A stereo view of the U-turn region, and **B**: the U6-A28-U23 base triple in the conserved core of the RNA–theophylline complex (Zimmermann et al., 1997). The dashed lines represent proposed hydrogen bonds in the structure (Zimmermann et al., 1997), and the arrow points to the N7 of residue A28 that, when modified to 7-deaza, showed much lower affinity for theophylline (see text).

the presence of a specifically bound metal. A metal-binding site was mapped onto the previously determined three-dimensional structure of the complex (Zimmermann et al., 1997) by identifying proton resonances specifically broadened in the presence of low concentrations of paramagnetic Mn^{2+} (Fig. 3). Figure 6 demonstrates that the proton resonances affected by Mn^{2+} ions are clustered in a tight turn within the theophylline-binding core of the complex. The metal (gray sphere) in Figure 6 was modeled qualitatively so that all the affected protons (white spheres) are close enough to the metal to account for the observed paramagnetic broadening, while also avoiding any steric overlap. The Mn^{2+}-titration experiments were carried out in a background of 2 mM free Mg^{2+}; therefore these results indicate that this site has higher affinity for Mn^{2+} than the other nonspecific metal-binding sites in the RNA. This is similar to class-I metal-binding sites observed in tRNA (Schimmel & Redfield, 1980), and metal-specific sites observed in ribosomal RNA by optical melting studies (Laing et al., 1994).

Although the NMR experiments performed here clearly identify a preferential Mn^{2+} site within the theophylline-binding core, these results do not address whether this is the site of the metal required for high-affinity theophylline binding.

The metal-binding site in the core of this RNA aptamer could perform a number of functions critical to theophylline binding and caffeine discrimination. By stabilizing the high density of negative charge created by the juxtaposition of multiple phosphate groups (C22, U23, U24, G25) in this turn (Fig. 6), the metal could facilitate folding of the core. This is a critical region in the core of the RNA because it allows interactions between conserved residues of the two internal loops (Fig. 1B) that are required for the formation of the ligand-binding pocket. Residues U24, G25, and G26 are part of the U-turn (Quigley & Rich, 1976; Jucker & Pardi, 1995; Zimmermann et al., 1997) that helps bring the upper and lower loops of the RNA together to form the ligand-binding site. Another potential role for the metal
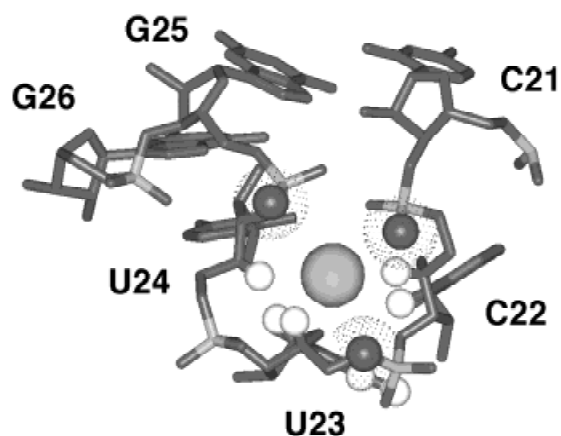
FIGURE 6. A model of the metal-binding site in the previously determined structure of the RNA–theophylline complex (Zimmermann et al., 1997). The gray sphere represents the divalent metal ion, and the white spheres indicate RNA proton resonances that are specifically broadened in the presence of 40 μM Mn^{2+} (Fig. 3). The van der Waals surface of phosphate oxygens that may coordinate the metal are stippled. The placement of the metal ion is not uniquely defined by the NMR data, and thus this picture shows one model consistent with the NMR data in the Mn^{2+}-titration (see text).

is to correctly orient the bases of residues C22 and U24 that hydrogen bond to theophylline, forming the critical base-triple that mediates the molecular discrimination of this RNA aptamer (Zimmermann et al., 1997). Although the data in Figures 3 and 6 clearly define the region of the metal-binding site, additional data such as thiophosphate interference-type experiments are needed to try to identify uniquely specific ligands on the RNA that are coordinating the metal.

Caffeine binding to the theophylline aptamer

One of the most striking features of this RNA aptamer is that it binds theophylline with a submicromolar K_d, while maintaining a 10,000-fold level of discrimination for caffeine (Jenison et al., 1994). This level of molecular discrimination is achieved because caffeine is incompatible with the central C22-theophylline-U24 base triple (Zimmermann et al., 1997). The N7-methyl group of caffeine breaks up the base triple sandwich and the associated favorable stacking interactions. In the absence of these stabilizing structural motifs, the theophylline-binding RNA is unable to maintain the active conformation of the ligand-binding site (Zimmermann et al., 1997).

The only stable interaction between caffeine and the theophylline aptamer detected by NMR spectroscopy is the stacking of the ligand on the terminal base pair of the RNA. This causes the G1 imino proton to become slowly exchanging, sharpens the resonance of the U32 imino proton, and is responsible for a small upfield shift of the G2 imino proton resonance (Fig. 4). These re-

sults were surprising because it was expected that some of the basic structural elements of the theophylline-binding core could form in the presence of caffeine. For example, the A5-G29 wobble pair does not interact directly with theophylline, and the U6-U23-A28 triple interacts with theophylline only through stacking interactions (Zimmermann et al., 1997). The fact that none of the core structural elements are observed suggests a cooperative folding mechanism for the RNA–theophylline complex, and that interactions of caffeine with the theophylline-binding core are too weak or transient in nature to be observed by NMR spectroscopy.

CONCLUSIONS

The three-dimensional structure of the RNA–theophylline complex revealed how interlocking structural motifs form a ligand-binding site that is able to discriminate theophylline from the highly similar molecule caffeine (Zimmermann et al., 1997). The functional group modification and mutational studies here showed that sequence changes outside the conserved core can still affect theophylline binding, and also confirmed the formation of the U-turn and the U6-A28-U23 base triple in the RNA–theophylline complex. This theophylline-binding RNA aptamer requires divalent metal for high-affinity binding. Indeed, a specific metal-binding site was located within the core of this RNA–theophylline complex using a paramagnetic Mn^{2+} titration. The proposed metal-binding site is part of the S-turn in the theophylline-binding pocket where the sugar–phosphate backbone makes a sharp bend, creating a large negatively charged surface. A titration study of the RNA aptamer with caffeine showed no evidence for theophylline binding in the conserved core, even at millimolar concentrations and a tenfold excess of caffeine to RNA. Instead, the caffeine appears to stack on the terminal base pair in the helix, distant from the theophylline-binding core, further demonstrating the high level of discrimination for this RNA aptamer.

MATERIALS AND METHODS

Sample preparation

The RNA samples for the NMR studies were generated by in vitro transcription using T7 RNA polymerase and synthetic DNA templates (Milligan et al., 1987; Milligan & Uhlenbeck, 1989). The uniformly ^{13}C/^{15}N-labeled sample of the Δ-33 RNA was prepared with ^{13}C/^{15}N-labeled NTPs as described (Batey et al., 1992; Nikonowicz et al., 1992). Pre-RNAs containing a 7-nt 3′-tail sequence (5′-GCAGGUC-3′) relative to the RNA shown in Figure 1B were transcribed and cleaved with a hammerhead ribozyme added in *trans* to produce a homogeneous-length RNA as described (Shields et al., 1999). After the cleavage reaction, the product RNA was separated from the pre-RNA by denaturing polyacrylamide gel electrophoresis purification, followed by a DEAE-Sephacel (Phar-

macia) anion-exchange chromatography. The final step in the production of the NMR sample was to dialyze the RNA extensively in the NMR buffer: 20 mM NaH_2PO_4, pH = 6.8, 30 mM NaCl, 2 mM $MgCl_2$ using a Centricon-3 concentrator (Amicon). Generally, 10–12 mL of buffer were passed over the RNA to insure complete equilibration of pH and Mg^{2+} ions. For the 1:1 RNA–theophylline complex, one equivalent of theophylline (Sigma-reference grade) was added to the sample. The sample was then lyophilized to dryness and finally resuspended in 350 μL of 90% H_2O/10% D_2O or 99.99% D_2O. For the NMR studies of the caffeine:RNA complex, 10 equivalents of caffeine were added to the purified RNA sample. After prolonged storage at 4 °C, samples were heated to 35 °C for 5 min in the NMR tube and then allowed to cool slowly to the experimental temperature.

NMR spectra of the manganese ion titration of RNA–theophylline complex

A two-dimensional (^{1}H,^{13}C) HSQC spectrum was collected on the uniformly ^{13}C/^{15}N-labeled RNA/theophylline complex in 20 mM NaH_2PO_4, pH = 6.8, 30 mM NaCl, 2 mM $MgCl_2$. A Mn^{2+} titration was performed by adding 5 μL aliquots of a concentrated $MnCl_2$ solution (in D_2O), and identical HSQC spectra were collected at total Mn^{2+} concentrations of 5, 10, 20, 25, 30, 35, and 40 μM. The concentration of the RNA–theophylline complex was therefore reduced by ~10% in the 40 μM added Mn^{2+} spectrum relative to the initial spectrum. Each spectrum was acquired in ~2 h with 512 complex points for 6,000 Hz in the ^{1}H dimension (t_2), and 190 complex points for 7,500 Hz in the indirect-^{13}C dimension (t_1) and used the States-TPPI method for quadrature detection in t_1 (Marion et al., 1989).

Binding-affinity measurements

The ΔTCT-4, Δ-31, Δ-33, and Δ-40 RNAs (see Fig. 1) used for comparing the effects of sequence variations outside the conserved core were generated by in vitro transcription as described above. The studies of the effects of different metals on theophylline binding were performed on the Δ-33 sample, also prepared by in vitro transcription. For the studies of the effects of 2′-deoxy or 7-deaza, 2′-deoxy substitutions on theophylline binding, the two separate strands shown in Figure 1C (and their mutants) were prepared by solid-phase synthesis and purified as previously described (Zimmermann et al., 1998). The individual strands were then combined in a 1:1 ratio to generate a theophylline-binding core containing the desired mutation. Equilibrium binding constants were determined for the wild-type and mutant theophylline-binding RNAs using the method of equilibrium filtration (Jenison et al., 1994; Zimmermann et al., 1998). Briefly, 20 nM ^{3}H-labeled theophylline was combined with the RNA of interest ranging in concentration from 0.05 to 10 μM in binding buffer: 100 mM HEPES (pH 7.3), 50 mM NaCl, and 5.0 mM $MgCl_2$. The complex was heated to 65 °C for 5 min and then cooled to 25 °C before being added (150 μL) to a Microcon-10 ultrafiltration spin column (Amicon). The spin columns containing the various concentrations of the RNA of interest were then briefly centrifuged, and aliquots (25 μL) were taken from above and below the ultrafiltration membrane. Scintillation counting re-

vealed the differential partitioning of the labeled ligand due to interaction with the RNA, and the data were fit to a single-site binding equation (Wyman & Gill, 1990). The binding constants measurements were performed in triplicate, and errors were estimated to be ~30%. For studies of theophylline binding in different metal ions, the pH was lowered to 6.8, and instead of adding $MgCl_2$, different divalent or lanthanide metals were added to give a solution of 5 mM metal ion.

REFERENCES

Allain FHT, Varani G. 1995. Divalent metal ion binding to a conserved wobble pair defining the upstream site of cleavage of group-I self-splicing introns. *Nucleic Acids Res 23*:341–350.

Batey RD, Inada M, Kujawinski E, Puglisi JD, Williamson JR. 1992. Preparation of isotopically labeled ribonucleotides for multidimensional NMR spectroscopy of RNA. *Nucleic Acids Res 20*:4515–4523.

Bertini I, Luchinat C. 1986. NMR of paramagnetic molecules in biological systems. Menlo Park, California: Benjamin/Cummings.

Dieckmann T, Suzuki E, Nakamura GK, Feigon J. 1996. Solution structure of an ATP-binding RNA aptamer reveals a novel fold. *RNA 2*:628–640.

Ellington AD, Szostak JW. 1990. In vitro selection of RNA molecules that bind specific ligands. *Nature 346*:818–822.

Fan P, Suri AK, Fiala R, Live D, Patel DJ. 1996. Molecular recognition in the FMN–RNA aptamer complex. *J Mol Biol 258*:480–500.

Feigon J, Dieckmann T, Smith FW. 1996. Aptamer structures from A to zeta. *Chem Biol 3*:611–617.

Gold L, Polisky B, Uhlenbeck O, Yarus M. 1995. Diversity of oligonucleotide functions. *Annu Rev Biochem 64*:763–797.

Heus HA. 1997. RNA aptamers. *Nat Struct Biol 4*:597–600.

Heus HA, Pardi A. 1991. Structural features that give rise to the unusual stability of RNA hairpins containing GNRA loops. *Science 253*:191–194.

Jenison RD, Gill SC, Pardi A, Polisky B. 1994. High-resolution molecular discrimination by RNA. *Science 263*:1425–1429.

Jiang F, Kumar RA, Jones RA, Patel DJ. 1996. Structural basis of RNA folding and recognition in an AMP-RNA aptamer complex. *Nature 382*:183–186.

Jiang L, Patel DJ. 1998. Solution structure of the tobramycin-RNA aptamer complex. *Nat Struct Biol 5*:769–774.

Jucker FM, Heus HA, Yip PF, Moors EHM, Pardi A. 1996. A network of heterogeneous hydrogen bonds in GNRA tetraloops. *J Mol Biol 264*:968–980.

Jucker FM, Pardi A. 1995. GNRA tetraloops make a U-turn. *RNA 1*:219–222.

Laing LG, Gluick TC, Draper DE. 1994. Stabilization of RNA structure by Mg ions. Specific and non-specific effects. *J Mol Biol 237*:577–587.

Marion D, Ikura M, Tschudin R, Bax A. 1989. Rapid recording of 2D NMR spectra without phase cycling—application to the study of hydrogen-exchange in proteins. *J Magn Reson 85*:393–399.

Milligan JF, Groebe DR, Witherell GW, Uhlenbeck OC. 1987. Oligoribonucleotide synthesis using T7 RNA polymerase and synthetic DNA templates. *Nucleic Acids Res 15*:8783–8789.

Milligan JF, Uhlenbeck OC. 1989. Synthesis of small RNAs using T7 RNA polymerase. *Methods Enzymol 180*:51–62.

Nikonowicz EP, Sirr A, Legault P, Jucker FM, Baer LM, Pardi A. 1992. Preparation of ^{13}C and ^{15}N labelled RNAs for heteronuclear multidimensional NMR studies. *Nucleic Acids Res 20*:4507–4513.

Osborne SE, Ellington AD. 1997. Nucleic acid selection and the challenge of combinatorial chemistry. *Chem Rev 97*:349–370.

Ott G, Arnold L, Limmer S. 1993. Proton NMR studies of manganese ion binding to tRNA-derived acceptor arm duplexes. *Nucleic Acids Res 21*:5859–5864.

Patel DJ. 1997. Structural analysis of nucleic acid aptamers. *Curr Opin Struct Biol 1*:32–46.

Quigley GJ, Rich A. 1976. Structural domains of transfer RNA molecules. *Science 194*:796–806.

Santa Lucia J, Kierzek R, Turner DH. 1992. Context dependence of hydrogen-bond free-energy revealed by substitutions in an RNA hairpin. *Science 256*:217–219.

Schimmel PR, Redfield AG. 1980. Transfer RNA in solution: Selected topics. *Annu Rev Biophys Bioeng 9*:181–221.

Shields TP, Mollova E, Marie LS, Hansen MR, Pardi A. 1999. High-performance liquid chromatography purification of homogenous-length RNA produced by *trans* cleavage with a hammerhead ribozyme. *RNA 5*:1259–1267.

Tuerk C, Gold L. 1990. Systematic evolution of ligands by exponential enrichment—RNA ligands to bacteriophage T4 DNA polymerase. *Science 249*:505–510.

Wilson DS, Szostak JW. 1999. In vitro selection of functional nucleic acids. *Annu Rev Biochem 68*:611–647.

Wyman J, Gill SJ. 1990. Binding and linkage. Functional chemistry of biological macromolecules. Mill Valley, California: University Science Books.

Yang Y, Kochoyan M, Burgstaller P, Westhof E, Famulok M. 1996. Structural basis of ligand discrimination by two related RNA aptamers resolved by NMR spectroscopy. *Science 272*:1343–1347.

Zimmermann GR, Jenison RD, Wick CL, Simorre J-P, Pardi A. 1997. Interlocking structural motifs mediate molecular discrimination by a theophylline-binding RNA. *Nat Struct Biol 4*:644–649.

Zimmermann GR, Shields TP, Jenison RD, Wick CL, Pardi A. 1998. A semiconserved residue inhibits complex formation by stabilizing interactions in the free state of a theophylline-binding RNA. *Biochemistry 37*:9186–9192.